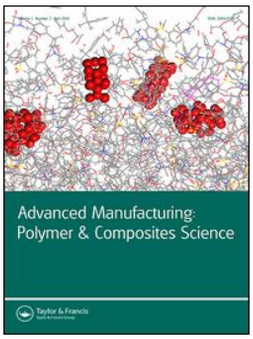

Taylor & Francis
Taylor & Francis Group

Advanced Manufacturing: Polymer & Composites Science

ISSN: 2055-0340 (Print) 2055-0359 (Online) Journal homepage: www.tandfonline.com/journals/yadm20

Parametric optimization of the processing of all-cellulose composite laminae

M. Mat Salleh, K. Magniez, S. Pang, J. W. Dormanns & M. P. Staiger

To cite this article: M. Mat Salleh, K. Magniez, S. Pang, J. W. Dormanns & M. P. Staiger (2017) Parametric optimization of the processing of all-cellulose composite laminae, Advanced Manufacturing: Polymer & Composites Science, 3:2, 73-79, DOI: 10.1080/20550340.2017.1324351

To link to this article: https://doi.org/10.1080/20550340.2017.1324351

Published online: 20 May 2017.

AMPCS Advanced Manufacturing: Polymer & Composites Science

Original Research Paper

Parametric optimization of the processing of all-cellulose composite laminae

M. Mat Salleh[1,2], K. Magniez[3], S. Pang[4], J. W. Dormanns[1] and M. P. Staiger*[,1]

[1]Department of Mechanical Engineering, University of Canterbury, Private Bag 4800, Christchurch 8140, New Zealand
[2]School of Manufacturing, Universiti Malaysia Perlis, Kampus Pauh Putra, Arau 02600, Perlis, Malaysia
[3]Institute for Frontier Materials, Deakin University, Locked Bag 20000, Geelong 3220, Victoria, Australia
[4]Department of Chemical and Process Engineering, University of Canterbury, Private Bag 4800, Christchurch 8140, New Zealand

Abstract Single-polymer composites based on cellulose I and/or II (*aka* all-cellulose composites) are emerging as a class of high-performance bio-based composite materials with mechanical properties suited to structural applications. There are various synthesis routes for the preparation of all-cellulose composites. However, little has been reported on the optimization of the processing variables affecting the properties of all-cellulose composites. In the present work, a range of all-cellulose composites were produced as single laminae via solvent infusion processing using a precursor of cellulose II fibers that were assembled as a woven 2D textile. The effects of dissolution time, dissolution temperature, and compaction pressure during hot pressing on the properties of the laminae were then systematically examined using a Taguchi design of experiment approach in order to identify the critical control factors. The tensile properties, fiber volume fraction, and crystallinity of the laminae were determined. Statistical analysis of variance and the signal-to-noise ratio were used to rank the importance of key control factors.

Keywords All-cellulose composites, Solvent infusion process, Design of experiments, Taguchi method, Analysis of variance

Cite this article M. Mat Salleh, K. Magniez, S. Pang, J. W. Dormanns and M. P. Staiger: *Adv. Manuf.: Polym. Compos. Sci.*, doi 10.1080/20550340.2017.1324351

Introduction

All-cellulose composite (ACC) materials are composed of a cellulose II matrix phase that is reinforced by cellulose I or II fibers or particulates. The concept of using the same polymer for both the reinforcement and matrix phases is aimed at facilitating the recyclability and improving mechanical performance of the final composite.[1] Nishino et al. first reported on the terminology, processing, and mechanical properties of ACCs.[2] ACCs may be produced with a relatively high elastic modulus (~20–30 GPa) and tensile strength (~120–500 MPa) depending on the chosen processing parameters.[2–4]

Gindl et al. first reported that ACCs may be manufactured by the partial (or selective) dissolution of cellulose I with a suitable solvent, where the portion of dissolved cellulose is then subsequently regenerated (via solvent exchange with a coagulant) to form a cellulose II matrix phase *in situ*.[5] Numerous control factors may influence the final mechanical properties of ACCs and these factors include: (a) the physicochemical properties of the cellulose precursor (e.g. crystal structure or polymorph, molecular weight, crystallinity); (b) dissolution conditions (e.g. type and relative amount of solvent, temperature, time, moisture content); (c) regeneration conditions (e.g. temperature, pressure, time, type and amount of coagulant); and (d) drying conditions (e.g. temperature, pressure, time).[6–14] In spite of the large array of control factors, the development of a systematic approach to optimization of processing-property relationships of ACCs has not yet been reported in literature.

Modern manufacturing frequently relies on design optimization (e.g. design of experiments (DOE)) in order to compete on the cost and performance of materials and products.[15] An example of a robust design optimization approach is the Taguchi methodology that has been previously used in optimizing the processing of both conventional and bio-based composite materials.[16–20] The construction of orthogonal arrays (OAs) as performed in a Taguchi experimental design enables the quantification of the effect of each control factor on various characteristic outputs (e.g. mechanical properties).[15,21] The Taguchi methodology allows identification of the most dominant control factors on chosen performance characteristics so that the non-dominant control factors can be ignored. Hence, a design optimization approach such as the Taguchi methodology is useful for studying the complex interdependencies between the above control factors in the manufacturing of ACCs.

ACCs may be fabricated as thin films (<1 mm thick) or laminated constructs with thicknesses up to 8–10 mm, leading to a range of potential applications.[1] However, an increase in the thickness of the ACCs also increases the likelihood of differential shrinkage and warpage of the final material. Generally, the solvent represents a relatively large volume (~80%) of

*Corresponding author, email: mark.staiger@canterbury.ac.nz

Received 20 December 2016; accepted 9 April 2017
DOI 10.1080/20550340.2017.1324351

Table 1 The selected control factors and their levels

	Levels		
Control factors	1	2	3
t_d (min)	30	60	90
T_d (°C)	95	105	115
σ_p (MPa)	0.25	0.5	1.0

Table 2 L9 orthogonal array with the levels of the control factors used in each of the 9 trials

Trial	t_d (min)	T_d (°C)	σ_p (MPa)
1	30	95	0.25
2	30	105	0.50
3	30	115	1.00
4	60	95	0.50
5	60	105	1.00
6	60	115	0.25
7	90	95	1.00
8	90	105	0.25
9	90	115	0.50

the cellulose–solvent solution that is subsequently removed during cellulose regeneration. Hence, significant volumetric shrinkage can be observed during the process from the precursor solution to the consolidated composite material. The application of pressure during processing of ACCs has been used to ensure consolidation and dimensional stability in the final material, adding yet another control factor in both the regeneration and drying stages.[10,22]

In the present work, the Taguchi methodology is implemented to quantify the impact of various control factors on the mechanical properties of ACCs produced via a laminate manufacturing route termed solvent infusion processing.[22] A preform (single or multiple woven or non-woven textile layers) is infused with a solvent through the application of a low vacuum pressure, similar in principle to vacuum-assisted resin transfer molding of conventional composites. Solvent infusion is then followed by temperature-triggered partial dissolution of the textile fibers *in situ*. The effect of the control factors on the microstructure was also investigated to gain greater understanding of the processing–structure–property relationships of ACCs.

Experimental procedures

Materials

A rayon fiber textile (Cordenka GmbH, Obernburg, Germany) in the form of a K2/2 twill weave was used. The textile was based on a multifilament yarn (Cordenka 700, 1840 dtex, f 1000) with a filament diameter of 12 μm and final areal weight of 450 g/m^2. The textile layers (120 (*l*) × 120 (*w*) mm) were dried under vacuum at 80 °C for 24 h prior to use. The ionic liquid, 1-butyl-3-methylimidazolium acetate (BmimAc) (BASIONIC™ BC 02, supplied by Sigma-Aldrich, St. Louis, USA), was dewatered under vacuum at 80 °C for 5 days prior to use.

Preparation of all-cellulose composite laminae

The ACC lamina was made using solvent infusion processing (SIP) which procedure has been described by Huber et al.[22] Briefly, a single layer of the textile was first placed on a flat plate mold covered with a bag, then it was vacuum and infused with BmimAc at room temperature (21 ± 2 °C). After this, the material–mold assembly was placed in a hot press for making a consolidated ACC lamina. The processing conditions investigated included dissolution time (t_d), dissolution temperature (T_d), and compaction pressure during hot pressing (σ_p) (Table 1). Once the hot pressing was completed, the material–mold assembly was cooled to room temperature (21 ± 2 °C) and the ACC lamina was then immersed in distilled water for a period of 3 days to regenerate the dissolved cellulose. The distilled water was replaced every 6 h over the first day to ensure rapid removal of the solvent, and replenished once daily over the second and third days. The resulting ACC lamina was then vacuum dried at 60 °C for 2 days under a pressure of 0.1 MPa.

Experimental design

The selection of control factors (t_d, T_d, and σ_p) and their levels as given in Table 1 were decided based on previous experimental findings.[7,10,22–26] It has been reported that the mechanical properties of ACCs increase with dissolution time (t_d) until a critical point after which the mechanical properties of ACCs may decrease due to the excessive dissolution of cellulose, resulting in an increased volume fraction of the matrix phase. Conversely, the formation of insufficient matrix phase at shorter t_d may lead to poor fiber–matrix adhesion that decreases the mechanical properties of the final ACC.[7]

It is also reported that an increase in dissolution temperature (T_d) would normally decrease the viscosity of the solvent, resulting in enhanced diffusion of the solvent into the cellulose textile that leads to more uniform dissolution of the cellulosic matrix and improved mechanical properties.[23] However, degradation of the cellulose molecule may occur if T_d is too high, resulting in a decrease in the mechanical properties of ACCs.[26] For instance, cellulose is thought to be degraded by most of the cellulose-dissolving ionic liquids at temperatures above ~150 °C.[27]

Huber et al. observed that increase in hot-pressing pressure (σ_p) improves the mechanical properties of ACCs, presumably due to a more uniform distribution and consolidation of the matrix phase that surrounds the undissolved fibers and the elimination of voids.[10] However, excessive pressure may force the cellulose fibers to separate that reduce the adhesion among fibers resulting in a decrease in the mechanical properties of ACCs.[23]

Using traditional design method, a full factorial experiment for three control factors and three levels would require 27 (3^3) trials. By comparison, according to the Taguchi fractional factorial experimental design, only nine trials are required to complete the experimental matrix.[28,29] An L_9 orthogonal array corresponds with the number of control factors and levels to be explored in this work (Table 2).

The Young's modulus (*E*) and ultimate tensile strength (UTS) are considered as "larger-the-better" quality characteristics in the context of a Taguchi analysis. Hence, the signal-to-noise ratio (*S*/*N*) was calculated using Equation (1).[28,30,31]

$$S/N = -10\log\left(\frac{1}{n}\sum_{i=1}^{n}\frac{1}{x^2}\right) \quad (1)$$

Table 3 Summary of the *E*, UTS and *S/N* values for the 9 trials. The standard deviation is indicated in parentheses

	Control factors						
Trials	t_d (min)	T_d (°C)	σ_p (MPa)	*E* (GPa)	*S/N*	UTS (MPa)	*S/N*
1	30	95	0.25	5.8 (0.04)	15.3	75.3 (0.17)	–22.5
2	30	105	0.5	5.9 (0.11)	15.4	74.2 (0.20)	–22.6
3	30	115	1.0	5.4 (0.15)	14.7	73.9 (0.15)	–22.6
4	60	95	0.5	7.1 (0.18)	17.0	76.9 (0.25)	–22.3
5	60	105	1.0	7.2 (0.19)	17.2	77.2 (0.18)	–22.3
6	60	115	0.25	7.3 (0.08)	17.3	77.7 (0.11)	–22.2
7	90	95	1.0	6.9 (0.14)	16.8	72.5 (0.14)	–22.8
8	90	105	0.25	6.8 (0.08)	16.7	71.8 (0.19)	–22.9
9	90	115	0.5	6.8 (0.12)	16.6	71.2 (0.12)	–23.0

where *n* is the number of measurements in each trial, *x* is the mechanical property value (*E* or UTS), and *S/N* ratio is in decibels (dB). Therefore, based on Equation (1), higher values of *x* will lead to a higher *S/N* ratio that consequently indicates greater influence of the control factor on the quality characteristic (i.e. *E* or UTS). The ANOVA parameters were also calculated, including the *F*-ratio (*F*), and percentage contribution (*P*). The most significant control factor was shown by the highest *P*. In addition, the comparison of *F* (ratio of the factor variance to the error variance) with the critical Fisher ratio (F_{crit}) can also be used to highlight significant control factors in the experimental design, where F_{crit} is determined from the *F* distribution table.

Mechanical testing

Tensile testing was carried out according to ASTM D3039[17] using an MTS Criterion Model C43.104 load frame equipped with a 2.5-kN load cell. Rectangular coupons (100 (*l*) × 10 (*w*) mm) were manually cut using a fresh razorblade. These samples were conditioned at 23 °C and 50% relative humidity (RH) for 24 h prior to testing at a constant crosshead speed of 2 mm/min. The samples were tested with a gauge length of 40 mm. Non-contact measurement of the strain was performed using a video extensometer (MTS FVX, TestWorks Axial/Transverse Video Extensometer with Video Traction software). The average *E* and UTS were based on five replicates.

Materials characterization

Microscopy samples were cut from ACC lamina into a rectangular shape with dimensions of (15 (*l*) × 6 (*w*) mm) and mounted in Epofix cold-setting embedding resin (Electron Microscopy sciences, Hatfield, PA, USA) according to the ASTM E3-11. An optimal surface for imaging by microscopy was obtained by manually removing a thin surface layer from the mounted sample using a fresh razorblade. The cold mounted samples were then vacuum dried at 95 °C overnight. Gold sputter-coated (180 s, 25 mA) samples were imaged using a JEOL7000F field emission scanning electron microscopy (FE-SEM) (JEOL Ltd., Tokyo, Japan) at an accelerating voltage of 5 kV. ImageJ software was used to measure the fiber (V_f), matrix (V_m), and void (V_v) volume fractions from the scanning electron micrographs.[32]

The phase composition and crystallinity of the final ACC lamina was determined by wide angle X-ray diffraction (WAXD) using an X-Pert Pro diffraction system. The CuK_α target (λ = 1.540598 Å) was excited with a voltage and current of 40 kV and 30 mA, respectively. Samples were analyzed using a scan step of 0.05° over the 2θ range of 5–50°. The crystallinity index (*CrI*) was calculated via the integral method,[33,34] where *CrI* is determined from the ratio of the area of the crystalline peak over that of the amorphous background using curve fitting software (Fityk, Version 0.9.8).[35] The amorphous background was calculated based on the data after Duchemin et al.[36] Integration of the fitted peaks and background (2θ = 10–40°) was carried out with MATLAB (R2014a, MathWorks, USA) in order to calculate *CrI* based on Equation 2. The crystallite size was also determined using the Scherrer equation (Equation 3).[37]

$$CrI = \frac{\text{Area}_{\text{crystalline}} - \text{Area}_{\text{amorphous}}}{\text{Area}_{\text{crystalline}}} \quad (2)$$

$$D = \frac{K\lambda}{\beta \cos\theta} \quad (3)$$

where D_{hkl} is the thickness of the crystallite perpendicular to the (*hkl*) plane, *K* is Scherrer's constant (0.9), λ is the wavelength of X-ray radiation, β is FWHM and θ is the diffraction angle.

Results and discussion

Taguchi and statistical analyses

The highest *E* and UTS are observed for Trial 6, while Trial 3 resulted in the lowest *E* and UTS (Table 3). A larger value of *S/N* indicates a greater influence of the control factor on ACC production. The highest *S/N* ratio for t_d and T_d on *E* are found at Level 2 (Figure 1). These results correlate with a t_d and T_d of 60 min and 105 °C, respectively (Table 1). The highest *S/N* ratio for t_d on UTS is observed at the same level as t_d on *E*. In contrast, the highest *S/N* ratio for T_d on UTS is found at Level 1 which correlates with a T_d of 95 °C (Table 1). The highest *S/N* ratio for σ_p on *E* and UTS is observed at the same level (Figure 1 and 2), corresponding with σ_p = 0.25 MPa (Table 1).

The optimal combination levels for maximizing *E* was at t_d, T_d, and σ_p of 60 min, 105 °C, and 0.25 MPa, respectively (Figure 1). Meanwhile, the optimal combination for maximizing UTS was at t_d, T_d, and σ_p of 60 min, 95 °C, and 0.25 MPa, respectively (Figure 2).

The above results are consistent with those reported in literature. Huber et al. reported that both *E* and UTS are affected by t_d and σ_p in a similar manner as shown in Figures 1 and 2.[22] From the SEM images (Figure 3), it is found that a reduction

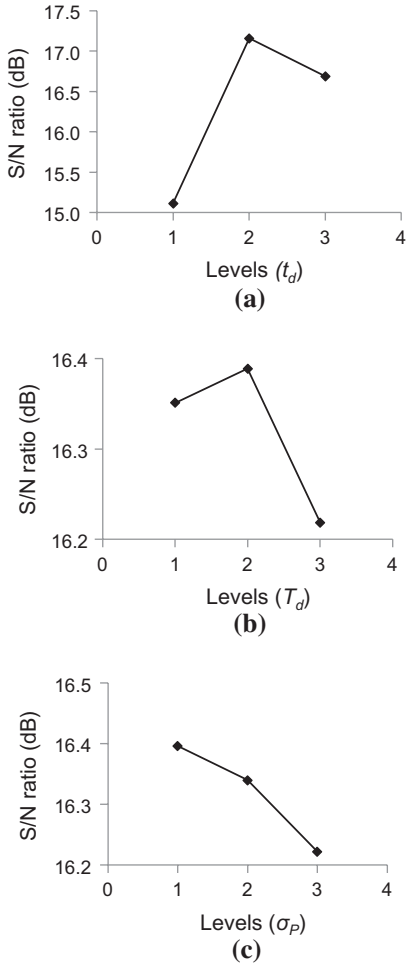

Figure 1 Response graphs for Young's modulus, showing the *S/N* ratio as a function of control factor level for dissolution time (a), dissolution temperature (b) and hot-pressing pressure (c)

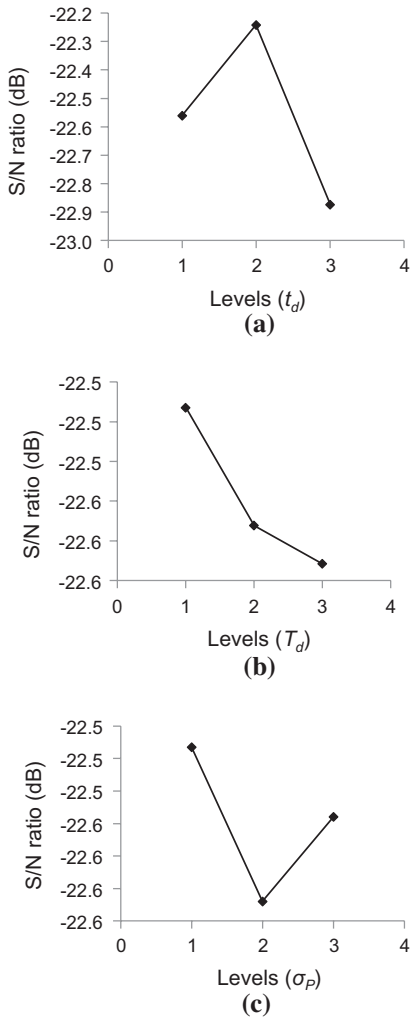

Figure 2 Response graphs for ultimate tensile strength, showing the *S/N* ratio as a function of control factor level for dissolution time (a), dissolution temperature (b) and hot-pressing pressure (c)

in t_d results in an increased presence of microvoids (Figure 3(a)), where the diameter of the microvoids is in the range of ~1–2 µm. The presence of microvoids is also concomitant with a reduction in the matrix phase that will reduce the transfer of load from the matrix to the fibers (Figure 4). However, the reinforcing and matrix phases that are both composed of cellulose II should not have greatly differing elastic moduli and thus loading sharing is not expected to play a critical role in the final mechanical properties of the ACC lamina. It is more likely that the presence of voids reduces the overall elastic modulus of the material and the critical stress required for the onset of failure. Further detailed investigation is required to observe the effects of voids on the *E* of ACC. The above observations are consistent with a 26 and 5.1% decrease in *E* and UTS with a change of t_d from 60 to 30 min, respectively (Table 3).

The microstructure in cross section comprised a uniform distribution of matrix phase that surrounds the fibers when processed with an optimal t_d and σ_p of 60 min and 0.25 MPa, respectively (Figure 3(b)). Under the above optimal processing conditions, *E* and UTS of the ACC were increased to 7.3 GPa and 77.7 MPa, respectively, (Table 3) due to enhanced homogeneity and consolidation of the ACC microstructure (Figure 3(b)).

The observation of widespread fiber–matrix interfacial failure tends to suggest that an interface or interphase exists in ACCs in spite of the fibers and matrix being chemically similar. A 6.8 and 7.6% decrease in *E* and UTS are observed with a change of t_d from 60 to 90 min, respectively (Table 3). Increased dissolution of the fibers is observed as t_d is increased as evidenced by an increase in V_m (Figure 4). A decrease in *E* and UTS is also observed in conjunction with an increase in V_v at a t_d of 30 or 90 min for the reasons as discussed above (Figure 4).

Although 10.0% matrix is often insufficient for wetting of fibers in conventional composites, the matrix is formed in all-cellulose composites *in situ*, resulting in the matrix phase being directly adjacent and in close proximity to the fiber surfaces, minimizing void formation due to insufficient wetting. It is asserted here that an interface and/or interphase do exist since failure does appear to emanate from the fiber–matrix boundary even in a microstructure in which most fibers are wetted by the matrix. It is also rare to observe a transverse failure of a fiber in spite of these ACCs consisting solely of cellulose II. The presence of an interphase and/or interface in ACCs remains to be clarified. The exact nature of the interface is still unknown in these materials. Attempts to characterize the interface/interphase region are hampered by experimental

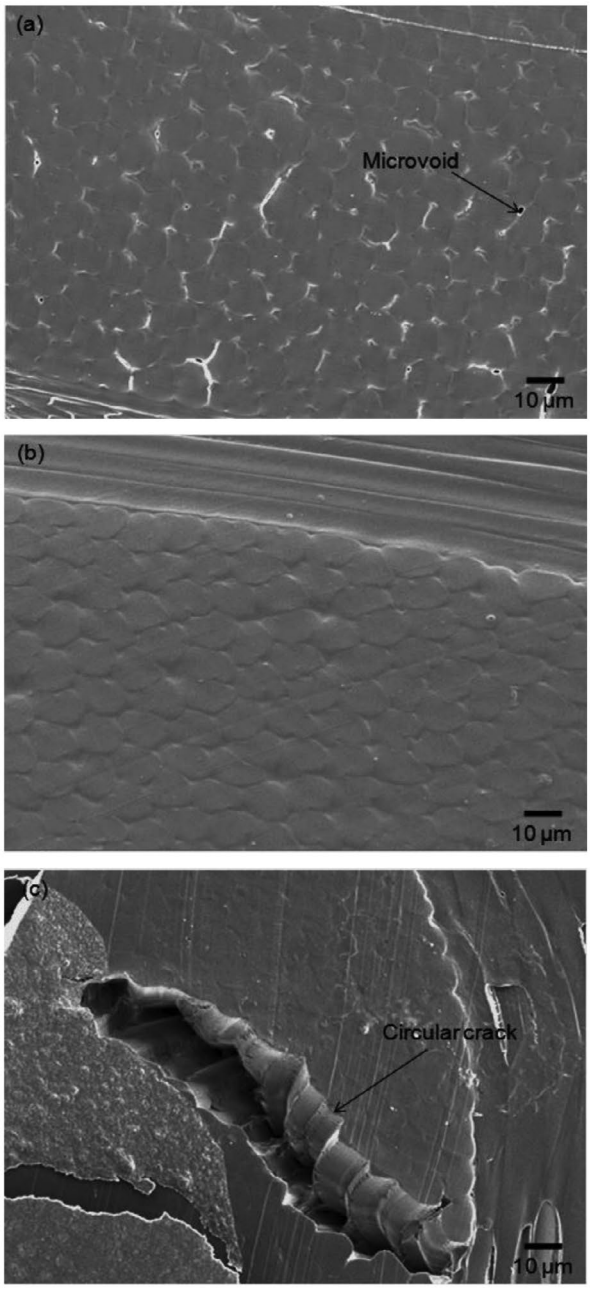

Figure 3 Scanning electron micrographs (SEM) of ACC laminae that were processed with dissolution times of (a) 30, (b) 60, and (c) 90 min

difficulties due to the small fraction of matrix phase that requires probing by nanoscale characterization methods.

According to the ANOVA results, t_d is the most significant control factor for both E and UTS as indicated by the highest P value (Tables 4 and 5) and $F > F_{crit}$. The relatively small influence of T_d on E and UTS could be due to the narrow T_d range used, although at higher T_d it would be necessary to verify that cellulose degradation does not take place. The lack of influence of T_d over E and UTS was indicated by the lowest P value (Table 4 and 5) and $F < F_{crit}$.

The optimal level of σ_p was identified as 0.25 MPa that corresponds closely with findings by Huber et al. (0.20 MPa).[22] However, σ_p appears to have a relatively small effect on E and UTS as indicated by a lower P (Tables 4 and 5) and $F < F_{crit}$.

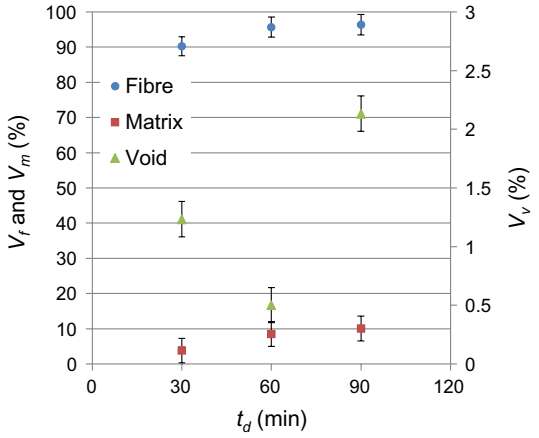

Figure 4 Fiber, matrix and void volume fractions as a function of dissolution time

Table 4 ANOVA results for Young's modulus

Control factor	*F*	*P* (%)	*S/N* differences	Significance
t_d	41.09	96.67	2.04	High
T_d	0.19	0.44	0.17	Weak
σ_p	0.22	0.51	0.18	Weak

*$F_{crit\ at\ 2,4}$ = 6.94.

Table 5 ANOVA results for ultimate tensile strength

Control factor	*F*	*P* (%)	*S/N* differences	Significance
t_d	84.38	95.2	0.63	High
T_d	1.33	1.50	0.07	Weak
σ_p	1.92	2.16	0.09	Weak

*$F_{crit\ at\ 2,4}$ = 6.94.

It is possible that a compaction pressure of 0.25 MPa during dissolution decreases the void content. An increase in σ_p increases the final mechanical properties of the ACC laminae, as previously discussed by Huber et al.[10] A fully consolidated composite laminates are possible with the addition of compaction pressure.[10] Further work that involves expanding the lower end range of the compaction pressure may be required.

Effect of dissolution time on the cellulose II structure

Generally, the *CrI* of the ACC lamina was found to increase from that of the as-received cellulose II textile (42%[10]) as shown by an increase in peak height and decrease in peak width in the (1 $\bar{1}$ 0) and (2 0 0) planes, respectively (Figure 5). An increase of *CrI* from 49.7 to 58.6% was observed with an increase in t_d from 30 to 90 min as calculated via the integral method according to Wakelin et al.[34] (Figure 6). An increase in *CrI* is likely to be due to the solvent selectively dissolving amorphous cellulose that subsequently regenerates into a more crystalline (or paracrystalline) phase.[22] In contrast, Soykeabkaew et al. report that *CrI* decreases with increasing t_d due to an increase in the fraction of amorphous phase under similar conditions to the present work.[7] An increase in the crystallite size was also observed with increasing t_d (Figure 6). The increase in crystallite size is

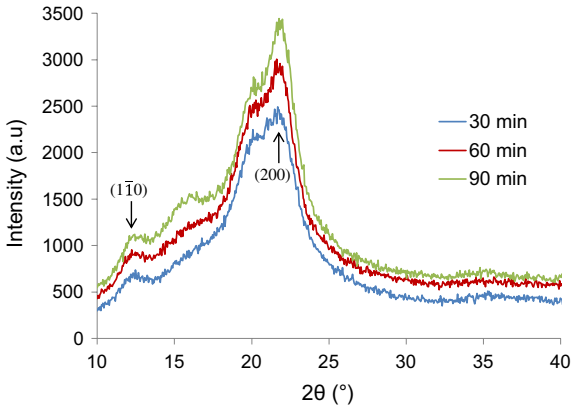

Figure 5 Wide angle X-ray diffractograms of ACC lamina as a function of the dissolution time using during processing

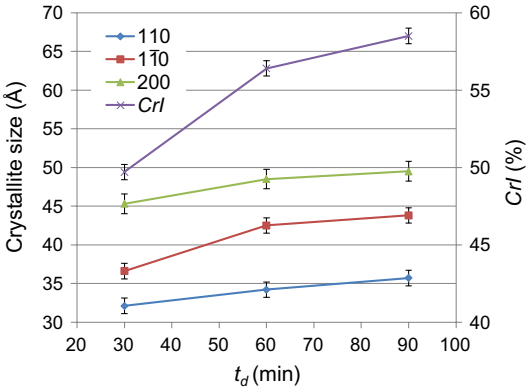

Figure 6 Crystallite size and crystallinity index in ACC lamina as a function of dissolution time, t_d

due to an increase in the lateral crystallite thickness perpendicular to the fiber axis.[38] Generally, the relationship between crystallite size and mechanical properties of ACC is inversely proportional in this present study which can be observed at t_d of 90 min. This finding is due to the increasing matrix fraction of ACCs at t_d of 90 min (Figure 4), resulting in the decreasing mechanical properties of ACCs. However, further works have to be done in order to obtain a better relationship between crystallite size and mechanical properties of ACCs.

Conclusions

The present study shows that it is possible to approach the optimization of all-cellulose composites through the use of a Taguchi-type analysis. The results of the Taguchi analysis could be correlated with microstructural changes that are found to be sensitive to the processing conditions used to fabricate an ACC laminae. The main conclusions that could be drawn from this study of ACC laminae are as follows:

- t_d imparts the greatest influence on *E* and UTS of ACC laminae as shown by a Taguchi fractional factorial experimental design and ANOVA. In contrast, σ_p and T_d had a relatively small effect on the mechanical properties of ACC laminae;
- A t_d of 60 min and σ_p of 0.25 MPa are found to be optimal in maximizing *E* and UTS of the final ACC laminae. The optimization of the mechanical properties was associated with a more homogeneous, void-free microstructure in the ACC laminae;
- An increase in *CrI* and crystallite size were observed with an increase in t_d in ACC laminae; and
- An increase of t_d up to 90 min results in a nonlinear, curved crack morphology due to an increase in V_f. The presence of microvoids is observed at a t_d of 30 min, leading to a decrease in *E* and UTS.

In future work, the authors will test the hypothesis that the optimization approach taken here may be applied to multiaxial all-cellulose laminates that are expected to be significantly different due to changes in failure mechanisms.

Acknowledgments

The authors are grateful to Mr. K. Stobbs and Mr. M. Flaws for technical assistance, and Dr. D. J. Pons for discussions regarding Taguchi analysis. One of the authors (MMS) gratefully acknowledges financial support provided by the Ministry of Higher Education Malaysia (MoHE) and Universiti Malaysia Perlis (UniMAP).

Disclosure statement

No potential conflict of interest was reported by the authors.

ORCID

M. P. Staiger http://orcid.org/0000-0002-1517-4404

References

1. T. Huber, J. Mussig, O. Curnow, S. Pang, S. Bickerton and M. P. Staiger: 'A critical review of all-cellulose composites', *J. Mater. Sci.*, 2012, **47**, 1171–1186.
2. T. Nishino, I. Matsuda and K. Hirao: 'All-cellulose composite', *Macromolecules*, 2004, **37**, 7683–7687.
3. C. Qin, N. Soykeabkaew, N. Xiuyuan and T. Peijs: 'The effect of fibre volume fraction and mercerization on the properties of all-cellulose composites', *Carbohyd. Polym.*, 2008, **71**, 458–467.
4. W. Gindl, K. J. Martinschitz, P. Boesecke and J. Keckes: 'Changes in the molecular orientation and tensile properties of uniaxially drawn cellulose films', *Biomacromolecules*, 2006, **7**, (11), 3146–3150.
5. W. Gindl and J. Keckes: 'All-cellulose nanocomposite', *Polymer*, 2005, **46**, 10221–10225.
6. R. Sescousse, K. A. Le, M. E. Ries and T. Budtova: 'Viscosity of cellulose–imidazolium-based ionic liquid solutions', *J. Phys. Chem. B*, 2010, **114**, (21), 7222–7228.
7. N. Soykeabkaew, N. Arimoto, T. Nishino and T. Peijs: 'All-cellulose composites by surface selective dissolution of aligned ligno-cellulosic fibres', *Compos. Sci. Technol.*, 2008, **68**, (10–11), 2201–2207.
8. H. Fink, P. Weigel, H. Purz and J. Ganster: 'Structure formation of regenerated cellulose materials from NMMO-solutions', *Prog. Polym. Sci.*, 2001, **26**, (9), 1473–1524.
9. M. Gericke, K. Schlufter, T. Liebert, T. Heinze and T. Budtova: 'Rheological properties of cellulose/ionic liquid solutions: from dilute to concentrated states', *Biomacromolecules*, 2009, **10**, (5), 1188–1194.
10. T. Huber, S. Pang and M. P. Staiger: 'All-cellulose composite laminates', *Compos. Part A*, 2012, **43**, (10), 1738–1745.
11. T. Nishino and N. Arimoto: 'All-cellulose composite prepared by selective dissolving of fiber surface', *Biomacromolecules*, 2007, **8**, 2712–2716.
12. R. P. Swatloski, S. K. Spear, J. D. Holbrey and R. D. Rogers: 'Dissolution of cellose with ionic liquids', *J. Am. Chem. Soc.*, 2002, **124**, 4974–4975.
13. A. Pinkert, K. N. Marsh, S. Pang and M. P. Staiger: 'Ionic liquids and their interaction with cellulose', *Chem. Rev.*, 2009, **109**, 6712–6728.
14. W. Gindl-Altmutter, J. Keckes, J. Plackner, F. Liebner, K. Englund and M. Laborie: 'All-cellulose composites prepared from flax and lyocell fibres compared to epoxy–matrix composites', *Compos. Sci. Technol.*, 2012, **72**, (11), 1304–1309.

15. R.K. Roy: 'A primer on the Taguchi method', 245; 2010, Dearborn, MI, Society of Manufacturing Engineers.
16. A. I. Azmi, R. J. T. Lin and D. Bhattacharyya: 'Parametric study of end milling glass fibre reinforced composites', Int. Conf. on 'Advances in materials and processing technologies', 2010, 1083–1088, Paris, France.
17. N. F. M. Rawi, K. Jayaraman and D. Bhattacharyya: 'A performance study on composites made from bamboo fabric and poly(lactic acid)', *J. Reinf. Plast. Compos.*, 2013, **32**, (20), 1513–1525.
18. A. Pourjavadi, M. Ayyari and M. Amini-Fazl: 'Taguchi optimized synthesis of collagen-g-poly(acrylic acid)/kaolin composite superabsorbent hydrogel', *Eur. Polym. J.*, 2008, **44**, (4), 1209–1216.
19. M. Cho, S. Bahadur and A. Pogosian: 'Friction and wear studies using Taguchi method on polyphenylene sulfide filled with a complex mixture of MoS2, Al2O3, and other compounds', *Wear*, 2005, **258**, (11–12), 1825–1835.
20. S. Baeten and I. Verpoest: 'Optimisation of a GMT-based cold pressing technique for low cost textile reinforced thermoplastic composites', *Compos. Part A: Appl. Sci. Manufac.*, 1999, **30**, (5), 667–682.
21. A. I. Azmi, R. J. T. Lin and D. Bhattacharyya: 'Machinability study of glass fibre-reinforced polymer composites during end milling', *Int. J. Adv. Manuf. Technol.*, 2012, **64**, 247–261.
22. T. Huber, S. Bickerton, J. Mussig, S. Pang and M. P. Staiger: 'Solvent infusion processing of all-cellulose composite materials', *Carbohyd. Polym.*, 2012, **90**, 730–733.
23. T. Huber: 'Processing of all cellulose composites via an ionic liquid route, PhD Thesis, Mechanical Engineering', 343; 2013, Christchurch, University of Canterbury.
24. N. Soykeabkaew, T. Nishino and T. Peijs: 'All-cellulose composites of regenerated cellulose fibres by surface selective dissolution', *Compos. Part A: Appl. Sci. Manufac.*, 2009, **40**, (4), 321–328.
25. N. Soykeabkaew: 'All-cellulose composite, in Department of Materials', 2007, London: University of London.
26. B. J. C. Duchemin, A. P. Mathew and K. Oksman: 'All-cellulose composites by partial dissolution in the ionic liquid 1-butyl-3-methylimidazolium chloride', *.Compos. Part A*, 2009, **40**, 2031–2037.
27. J. L. Anderson, D. W. Armstrong and G.-T. Wei: 'Ionic liquids in analytical chemistry', *Anal. Chem.*, 2006, **78**, (9), 2892–2902.
28. P.J. Ross: 'Taguchi techniques for quality engineering', Vol. 2nd edn, 322–327; 1996, New York: McGraw-Hill.
29. A. I. Azmi: 'Machinability study of fibre-reinforced polymer matrix composites, in Centre for Advanced Composite Materials', 2012, Auckland: University of Auckland.
30. Taguchi, G., S. Chowdhury, and Y. Wu: 'Taguchi's quality engineering handbook', 2005, Hoboken, NJ: Wiley-Interscience.
31. R. K. Roy: 'Design of experiments using the Taguchi approah: 16 steps to product and process improvement', 2001, New York, Wiley.
32. Rasband, W.: 'ImageJ, US National Institutes of Health', 1997, 2012, Bethesda, MD, http:\\imagej.nih.gov/ij.
33. L. Segal, J. J. Creely, A. E. Martin and C. M. Conrad: 'An empirical method for estimating the degree of crystallinity of native cellulose using the X-ray diffractometer', *Text. Res. J.*, 1959, **29**, (10), 786–794.
34. J. H. Wakelin, H. S. Virgin and E. Crystal: 'Development and comparison of two X-ray methods for determining the crystallinity of cotton cellulose', *J. Appl. Phys.*, 1959, **30**, (11), 1654–1662.
35. M. Wojdyr: 'Fityk: a general-purpose peak fitting program', *J. Appl. Crystallogr.*, 2010, **43**, (5), 1126–1128.
36. B. Duchemin, A. Thuault, A. Vicente, B. Rigaud, C. Fernandez and S. Eve: 'Ultrastructure of cellulose crystallites in flax textile fibres', *Cellulose*, 2012, **19**, (6), 1837–1854.
37. I. Nieduszynski and R. Preston: 'Crystallite size in natural cellulose', *Nature*, 1970, **225**, 273–274.
38. R. Ibbett, D. Domvoglou and D. Phillips: 'The hydrolysis and recrystallisation of lyocell and comparative cellulosic fibres in solutions of mineral acid', *Cellulose*, 2008, **15**, (2), 241–254.